Efficient Method for Solving TM-Polarized Plane Wave Scattering from Two-Dimensional Perfect Conductor Surfaces Using Fourier Series Approximation of the Green's Function

Mohammad AHMAD

Dept. of Electrical and Computer Engineering, University of Massachusetts, Dartmouth, USA

mahmad1@umassd.edu

Submitted July 26, 2021 / Accepted September 2, 2021

Abstract. *The method of moments generates a matrix which is usually solved using iterative methods due to the high computational complexity of a direct inversion. The cost of matrix-vector multiplications and memory requirement at each iteration step is proportional to $O(N^2)$, where N is the number of unknowns in the problem. To reduce the computational complexity, the Green's function is approximated using Fourier series. This will allow to separate the source points from the observation points. Hence, aggregate all source points and then multiply it with each observation point with a small adjustment in the aggregation term. The proposed method is tested by solving electromagnetic wave scattering from perfect conductor two-dimensional basic canonical shape, i.e., circular cylinder. The results showed that the proposed method is accurate and for large N it has a computational complexity less than the direct matrix-vector multiplication.*

Keywords

Electromagnetic wave scattering, Fourier series, method of moments, perfect conductor surfaces, two-dimensional

1. Introduction

Method of moments (MoM) is a numerical method that is used to solve boundary-integral equations [1] and produces a matrix. The direct inversion for the matrix is limited to small scale problems due to the high numerical cost. Hence, iterative methods are found to be numerically more effective [2] where matrix-vector multiplication (MVM) count and memory requirement (MR) are proportional to $O(N^2)$ at each iteration step where N is the number of unknowns in the problem.

For the last several decades, two major groups of algorithms have been developed to decrease the numerical demands of MVM and the associated MR. The first group is the algebra-based methods such as the adaptive cross-approximation algorithm [3], [4], the multilevel matrix decomposition method [5], and the IE-QR algorithm [6]. They are kernel independent and improve the computational complexity through linear-algebra manipulations on the MoM matrix. The second group is the kernel-based methods. Their implementations, performances, and constructions depend on the specific integral kernels. This group uses two ideas. The first idea depends on the grid representation to enable the use of the fast Fourier transform (FFT) to solve the MoM matrix. One old and simple method is a conjugate gradient fast Fourier transform [7], [8]. It reduces the MVM operation count and MR proportional to $O(N\log N)$ and $O(N)$, respectively. However, this method does not work with all kinds of basis functions and hence its application is restricted [9]. To solve this issue, an adaptive integral method was developed which reduces the MVM operation count proportional to $O(N^{3/2}\log N)$ operations and the MR proportional to $O(N^{3/2})$ [10], [11]. This method uses arbitrary basis functions that are projected on a uniform grid to enable the use of FFT. A similar idea is also employed in the precorrected–FFT [12], [13], sparse-matrix/canonical grid [14], and integral equation–FFT methods [15]. The other idea is to replace the Green's function with an equivalent mathematical representation that separates the observation point from the source point. The most well-known method to adapt this idea is the fast multipole method (FMM) which reduces both MVM and MR to $O(N^{3/2})$ [16], [17]. The multilevel version of FMM reduces numerical complexity to $O(N\log N)$ [18]. Several enhancements, adjustments, and approaches have been done or based on the conventional FMM over the years [19–24]. However, all [16–24] methods require intensive derivation to separate the observation point from the source point and sometimes it is impossible which make these methods useless. In addition, even though the methods [3–6] and [9–24] introduce additional parameters on the MoM which will lead to increase the difficulty of the algorithm, their efficiency improves as N increases. Note MoM is usually used to solve problems that require millions of unknowns or more.

In this paper, the Green's function is replaced with the Fourier series (FS) approximation. This method will be called the Fourier series method of moments (FS-MoM). The resultant equation separates the observation point from the source point without any additional effort and regardless of the Green's function. Therefore, all source points will be aggregated and then multiplied by each observation point with a small adjustment to the aggregation term. The advantages of this approach are efficiency, accuracy, generality, and simplicity.

The outline of this paper is as follows. An FS representation analysis for two-dimensional (2D) function and an FS representation of the 2D Green's function for electromagnetic wave scattering (EWS) is described in Sec. 2.1. Section 2.2 discusses how the FS-MoM is incorporated with MoM to reduce the computational complexity. Finally, Section 3 presents the numerical results to validate the proposed method, comparison, and discussion when the FS-MoM and MoM are applied to solve the EWS from perfect electric conductor (PEC) basic canonical shape, i.e., circular cylinder.

2. Formulation of the Problem

2.1 Fourier Series Representation Analyses

Assume that $f(x,y)$ is piecewise continuous on $[-L_x/2 \le x \le L_x/2]$ in the x-direction and on $[-L_y/2 \le y \le L_y/2]$ in the y-direction where L_x and L_y are constants. The FS representation of $f(x,y)$ is given by [25]

$$f(x,y) = \sum_{n_y=-\infty}^{\infty} \sum_{n_x=-\infty}^{\infty} C_{n_y n_x} \cdot \mathrm{e}^{\mathrm{j}n_x\omega_{0_x}x} \cdot \mathrm{e}^{\mathrm{j}n_y\omega_{0_y}y} \tag{1}$$

where

$$C_{n_y n_x} = \frac{1}{T_{0_y}} \frac{1}{T_{0_x}} \int_{-T_y/2}^{T_y/2} \int_{-T_x/2}^{T_x/2} f(x,y) \cdot \mathrm{e}^{-\mathrm{j}n_x\omega_{0_x}x} \cdot \mathrm{e}^{-\mathrm{j}n_y\omega_{0_y}y} \,\mathrm{d}x\mathrm{d}y \tag{2}$$

is the Fourier coefficient, $T_{0_x} \ge L_x$, $T_{0_y} \ge L_y$, $\omega_{0_x} = 2\pi/T_{0_x}$ and $\omega_{0_y} = 2\pi/T_{0_y}$.

For 2D EWS, the Green's function is the zeroth-order Hankel function of the second kind $f(x,y) = H_0^{(2)}(k_0|\boldsymbol{\rho}|)$ [9] where $k_0 = 2\pi/\lambda$ is the wavenumber, λ is the wavelength and $\boldsymbol{\rho} = x\mathbf{a}_x + y\mathbf{a}_y$. The FS representation for it using (1) is

$$\begin{aligned} f(x,y) &= H_0^{(2)}\left(k_0|\boldsymbol{\rho}|\right) = H_0^{(2)}\left(k_0\sqrt{x^2+y^2}\right) \\ &= \underbrace{\sum_{n_y=-N_y}^{N_y} \sum_{n_x=-N_x}^{N_x} C_{n_y n_x} \cdot \mathrm{e}^{\mathrm{j}n_x\omega_{0_x}x} \cdot \mathrm{e}^{\mathrm{j}n_y\omega_{0_y}y}}_{f_N(x,y)} + \mathrm{TR} \end{aligned} \tag{3}$$

where N_x and N_y are the upper limits of the summations, TR is the truncation error, and $f_N(x,y)$ is the approximation of $f(x,y)$ when the summations are truncated by N_x and N_y. Equation (3) is valid in the domain of the solution except when $\boldsymbol{\rho} = 0$. Truncation error arises in (3) due to replace the $\pm\infty$ limits in the summations by N_x and N_y. Limits of the summations can be determined for the required mean square error (MSE) using [25]

$$\mathrm{MSE} = \frac{1}{T_{0_y}} \frac{1}{T_{0_x}} \int_{-T_y/2}^{T_y/2} \int_{-T_x/2}^{T_x/2} \mathrm{TR}^2(x,y) \,\mathrm{d}x\mathrm{d}y$$

where $\mathrm{TR} = f(x,y) - f_N(x,y)$.

Note is that the Fourier transform ($\mathcal{F}$) for 2D Green's function is given by [26]

$$\tilde{H}_0^{(2)}\left(k_x, k_y\right) = \mathcal{F}\left\{H_0^{(2)}\left(k_0|\boldsymbol{\rho}|\right)\right\} = \frac{4\mathrm{j}}{k_y^2 + k_x^2 - k_0^2} \tag{4}$$

where k_x and k_y are the Fourier variables. Therefore, equation (4) can be used to evaluate the Fourier coefficient $C_{n_x n_y}$ as

$$C_{n_y n_x} = \frac{1}{T_{0_y}} \frac{1}{T_{0_x}} \tilde{H}_0^{(2)}\left(n_x\omega_{0_x}, n_y\omega_{0_y}\right). \tag{5}$$

Using (4) instead of (2) will significantly reduce the load of calculate the Fourier coefficient.

2.2 Incorporating FS-MoM in MoM

Consider a problem of a scalar wave produced by a source $\mathbf{E}_z^{\mathrm{inc}}$ in the presence of a 2D arbitrarily PEC shaped object centered at the origin and having maximum length of L_x in the x-direction and maximum length of L_y in the y-direction immersed in free space as shown in Fig. 1.

Assume that both the source and the object have no variation along the z-axis. The solution of the electric field integral equation (EFIE) for this case with TM^z polarizing using MoM is given by [9]

$$\mathbf{E} = \mathbf{ZI} \tag{6}$$

where $\mathbf{Z}$ is the impedance matrix given by [9]

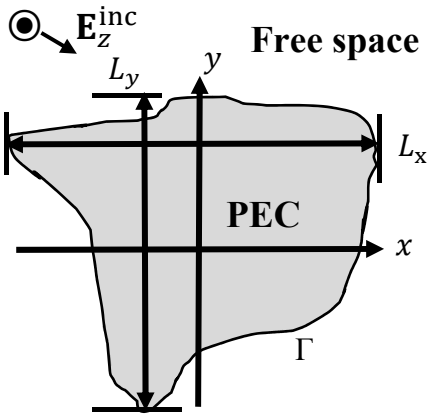

Fig. 1. A cylindrical PEC contour of constant cross section and extending infinitely in the $\pm z$ direction.

$$Z_{mn} = \frac{k_0\eta_0}{4}\int_\Gamma t_m(\boldsymbol{\rho})\,\mathrm{d}\Gamma\int_\Gamma H_0^{(2)}\left(k_0\left|\boldsymbol{\rho}-\boldsymbol{\rho}'\right|\right) f_n(\boldsymbol{\rho}')\,\mathrm{d}\Gamma' \quad (7)$$

where Γ denotes the boundary enclosing the scatterer, $\boldsymbol{\rho} = x\mathbf{a}_\mathrm{x} + y\mathbf{a}_\mathrm{y}$ and $\boldsymbol{\rho}' = x'\mathbf{a}_\mathrm{x} + y'\mathbf{a}_\mathrm{y}$ denote the observation and the source point respectively, $\boldsymbol{\rho}$ and $\boldsymbol{\rho}' \in \Gamma$, $t_m(\boldsymbol{\rho})$ denotes the testing functions, $f_n(\boldsymbol{\rho}')$ denotes the basis functions, and η_0 is the free space impedance, $\mathbf{E} = [E_\mathrm{z}^{\mathrm{inc}(1)} \ldots E_\mathrm{z}^{\mathrm{inc}(m)} \ldots E_\mathrm{z}^{\mathrm{inc}(N)}]$ is a column vector where $E_z^{\mathrm{inc}(m)} = \int_\Gamma t_m(\boldsymbol{\rho})\,\mathbf{E}_\mathrm{z}^{\mathrm{inc}}(\boldsymbol{\rho})\,\mathrm{d}\Gamma$, and $\mathbf{E}_\mathrm{z}^{\mathrm{inc}}(\boldsymbol{\rho}) = E_0\exp(\mathrm{j}k_0(x\cos\Phi_\mathrm{i} + y\sin\Phi_\mathrm{i}))$ is the known incident electric field, E_0 is a constant, and Φ_i is the incident angle, $\mathbf{I} = [I_1 \ldots I_n \ldots I_N]$ is a column vector to be determined and the relation between it and the unknown current is $J(\boldsymbol{\rho}) = \sum_{n=1}^{N} I_n f_n(\boldsymbol{\rho})$.

Approximate the Green's function in (7) using (1) yields

$$H_0^{(2)}\left(k_0\left|\boldsymbol{\rho}-\boldsymbol{\rho}'\right|\right) = H_0^{(2)}\left(k_0\sqrt{(x-x')^2+(y-y')^2}\right) = \sum_{n_\mathrm{y}=-N_\mathrm{y}}^{N_\mathrm{y}}\sum_{n_\mathrm{x}=-N_\mathrm{x}}^{N_\mathrm{x}} C_{n_\mathrm{y}n_\mathrm{x}}\,\mathrm{e}^{\mathrm{j}n_\mathrm{x}\omega_{0\mathrm{x}}x}\,\mathrm{e}^{\mathrm{j}n_\mathrm{y}\omega_{0\mathrm{y}}y}\cdot\mathrm{e}^{-\mathrm{j}n_\mathrm{x}\omega_{0\mathrm{x}}x'}\,\mathrm{e}^{-\mathrm{j}n_\mathrm{y}\omega_{0\mathrm{y}}y'} + \mathrm{TR} \quad (8)$$

where $T_{0\mathrm{x}} = 2L_\mathrm{x}$ and $T_{0\mathrm{y}} = 2L_\mathrm{y}$ to cover all the possible values of $|\boldsymbol{\rho} - \boldsymbol{\rho}'|$. Equation (8) is valid in the domain of the solution except when $\boldsymbol{\rho} - \boldsymbol{\rho}' = 0$. If (2) is used to evaluate $C_{n\mathrm{x}n\mathrm{y}}$, $f(x,y)$ that is required in (2) is $f(x,y) = H_0^{(2)}\left(k_0\sqrt{x^2+y^2}\right)$.

For FS-MoM, incorporating (8) with (7) and then incorporate into (6) yields

$$\begin{aligned} E_\mathrm{z}^{\mathrm{inc}}(\rho_m) &= \sum_{n=1}^{N} Z_{mn} I_n \\ &= \frac{k_0\eta_0}{4}\sum_{n_y=-N_\mathrm{y}}^{N_\mathrm{y}}\sum_{n_\mathrm{x}=-N_\mathrm{x}}^{N_\mathrm{x}} C_{n_\mathrm{y}n_\mathrm{x}} \\ &\times\int_\Gamma t_m(\boldsymbol{\rho})\,\mathrm{e}^{\mathrm{j}n_\mathrm{x}\omega_{0\mathrm{x}}x}\,\mathrm{e}^{\mathrm{j}n_\mathrm{y}\omega_{0\mathrm{y}}y}\,\mathrm{d}\Gamma \\ &\times\sum_n\int_\Gamma f_n(\boldsymbol{\rho}')\,\mathrm{e}^{-\mathrm{j}n_\mathrm{x}\omega_{0\mathrm{x}}x'}\,\mathrm{e}^{-\mathrm{j}n_\mathrm{y}\omega_{0\mathrm{y}}y'}\,\mathrm{d}\Gamma'\,I_n. \end{aligned} \quad (9)$$

This approach, i.e., (9), can be used. However, note that the Green's function, i.e., $H_0^{(2)}(k_0|\boldsymbol{\rho}|)$ goes to infinity when $(k_0|\boldsymbol{\rho}|)$ goes to zero. As the result, high values for the upper limits in (9) are required. Therefore, to reduce the values of the upper limits which will lead to reduce the computational complexity for the proposed method, rather than use the FS-MoM for the whole interval, it will be used for $(k_0|\boldsymbol{\rho}|) > (k_0|\bar{\boldsymbol{\rho}}|)$ where $|\bar{\boldsymbol{\rho}}|$ is a none zero constant where the FS-MoM starts. Hence, this method will use a combination of direct multiplication for $(k_0|\boldsymbol{\rho}|) < (k_0|\bar{\boldsymbol{\rho}}|)$ and fast multiplication, i.e., FS-MoM for $(k_0|\boldsymbol{\rho}|) > (k_0|\bar{\boldsymbol{\rho}}|)$. Therefore, (6) becomes

$$\mathbf{E} = \mathbf{ZI} = \underbrace{\mathbf{ZI}}_{\substack{\text{direct}\\ \text{multiplication}}} + \underbrace{\mathbf{ZI}}_{\substack{\text{fast}\\ \text{multiplication}}},$$

$$E_\mathrm{z}^{\mathrm{inc}}(\rho_m) = \sum_{n=1}^{N} Z_{mn} I_n = \sum_{n\in|\boldsymbol{\rho}-\boldsymbol{\rho}'|<|\bar{\boldsymbol{\rho}}|} Z_{mn} I_n + \frac{k_0\eta_0}{4}\sum_{n_\mathrm{y}=-N_\mathrm{y}}^{N_\mathrm{y}}\sum_{n_\mathrm{x}=-N_\mathrm{x}}^{N_\mathrm{x}} C_{n_\mathrm{y}n_\mathrm{x}} \times\int_\Gamma t_m(\boldsymbol{\rho})\,\mathrm{e}^{\mathrm{j}n_\mathrm{x}\omega_{0\mathrm{x}}x}\,\mathrm{e}^{\mathrm{j}n_\mathrm{y}\omega_{0\mathrm{y}}y}\,\mathrm{d}\Gamma \times \sum_{n\in|\boldsymbol{\rho}-\boldsymbol{\rho}'|>|\bar{\boldsymbol{\rho}}|}\int_\Gamma f_n(\boldsymbol{\rho}')\,\mathrm{e}^{-\mathrm{j}n_\mathrm{x}\omega_{0\mathrm{x}}x'}\,\mathrm{e}^{-\mathrm{j}n_\mathrm{y}\omega_{0\mathrm{y}}y'}\,\mathrm{d}\Gamma' I_n \quad (10)$$

where $|\bar{\boldsymbol{\rho}}|$ is the value where fast multiplication starts.

The implementation of (10) is done as follows. First, determine the first observation point ($m = 1$) and then divide the source points into two groups, one corresponding to direct multiplication using $n \in |\boldsymbol{\rho} - \boldsymbol{\rho}'| < |\bar{\boldsymbol{\rho}}|$ and the other to fast multiplication using $n \in |\boldsymbol{\rho} - \boldsymbol{\rho}'| > |\bar{\boldsymbol{\rho}}|$. Second, multiply the unknown currents with its source points using

$$Aggregation_{|m=1} = \sum_{n\in|\boldsymbol{\rho}-\boldsymbol{\rho}'|>|\bar{\boldsymbol{\rho}}|}\int_\Gamma f_n(\boldsymbol{\rho}')\,\mathrm{e}^{-\mathrm{j}n_\mathrm{x}\omega_{0\mathrm{x}}x'}\,\mathrm{e}^{-\mathrm{j}n_\mathrm{y}\omega_{0\mathrm{y}}y'}\,\mathrm{d}\Gamma' I_n.$$

Third, for the first observation point, evaluate the direct multiplication using $\sum_{n\in|\boldsymbol{\rho}-\boldsymbol{\rho}'|<|\bar{\boldsymbol{\rho}}|} Z_{1n} I_n$ and fast multiplication using

$$\frac{k_0\eta_0}{4}\sum_{n_\mathrm{y}=-N_\mathrm{y}}^{N_\mathrm{y}}\sum_{n_\mathrm{x}=-N_\mathrm{x}}^{N_\mathrm{x}} C_{n_\mathrm{y}n_\mathrm{x}} \times\int_\Gamma t_1(\boldsymbol{\rho})\,\mathrm{e}^{\mathrm{j}n_\mathrm{x}\omega_{0\mathrm{x}}x}\,\mathrm{e}^{\mathrm{j}n_\mathrm{y}\omega_{0\mathrm{y}}y}\,\mathrm{d}\Gamma \times Aggregation_{|m=1}.$$

Forth, for the next observation point ($m = 2$), adjust the $Aggregation_{|m=1}$ component that has been found in the second step to accommodate the new observation point. Few components which were in the direct multiplication group may now be in the fast multiplication group and vice versa. Repeat the third step for $m = 2$. Finally, for each new observation point, keep adjusting the previous aggregation components and then repeat the third step until the last observation point $m = N$.

Table 1 shows the computational complexity for FS-MoM.

3. Results and Discussion

In this section, the FS-MoM method is validated first by comparing the Green's function, i.e., $H_0^{(2)}(k_0|\boldsymbol{\rho}|)$, with its FS representation, i.e., (3), and calculating the MSE between them. Then, the proposed method, i.e., (10), is used to solve EWS from canonical 2D shape, i.e., circular cylinder, with different sizes and MSE with MoM, i.e., (6), as a reference is calculated as a function of the upper limits of the summations and number of points on the scatterer. A comparison of the time and memory required to perform MVM are shown for the two methods. The results demonstrate the numerical complexity and accuracy of the proposed method.

N: number of total basis functions.	FS-MoM N_x and N_y: upper summation limits for the 2D FS-MoM. N_{direct}: number of points that are going to multiply directly in the FS-MoM method. $N_{fast} = N - N_{direct}$: number of points that are going to multiply efficiency using the FS-MoM method.	
	Term	Computational Complexity
Near-field interactions	$\sum_{n\in\lvert\boldsymbol{\rho}-\boldsymbol{\rho}'\rvert<\lvert\bar{\boldsymbol{\rho}}\rvert} Z_{mn} I_n$	$N \times N_{direct}$
Aggregation	$\sum_{n\in\lvert\boldsymbol{\rho}-\boldsymbol{\rho}'\rvert>\lvert\bar{\boldsymbol{\rho}}\rvert} \int_\Gamma f_n(\boldsymbol{\rho}') \times e^{-jn_x\omega_{0_x}x'} e^{-jn_y\omega_{0_y}y'} d\Gamma' I_n$	$(2N_y+1)\times(2N_x+1)N_{fast}$
Fourier coefficient	$\sum_{n_y=-N_y}^{N_y} \sum_{n_x=-N_x}^{N_x} C_{n_y n_x}$	$(2N_y+1)\times(2N_x+1)$
Disaggregation	$\int_\Gamma t_m(\boldsymbol{\rho}) \times e^{jn_x\omega_{0_x}x} e^{jn_y\omega_{0_y}y} d\Gamma \times (\bullet)$	$(2N_y+1)\times(2N_x+1)N$
Computational complexity =(sum of all columns)	$N \times N_{direct} + (2N_y+1)(2N_x+1)\times[N_{fast}+1+N]$	

Tab. 1. Computational complexity for FS-MoM.

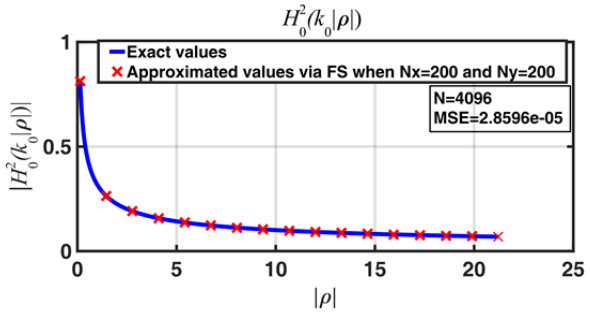

Fig. 2. The zeroth-order Hankel function of the second kind as a function of |ρ| and the FS approximation.

First, (3) is used to approximate the Green's function $f(x,y) = H_0^{(2)}\left(k_0\sqrt{x^2+y^2}\right)$ to validate the proposed method. Figure 2 shows the magnitude of the Hankel function versus $|\boldsymbol{\rho}|$ and the FS approximate for it where $0.1 < |\boldsymbol{\rho}| \le 22$, $N = 4096$ is the number of points in the interval, and $\lambda = 1$ is used. Also, the value of $N_x = 200$, $N_y = 200$, and MSE = 2.8596×10^{-5} are shown.

For the next results, the following assumptions are used. First, the iterative method that is used in this section is the conjugate gradient method [2]. Second, $(k_0|\boldsymbol{\rho}|) > (0.55) = (k_0|\bar{\boldsymbol{\rho}}|)$ is used. Third, $E_0 = 1$ and $\Phi_i = 0$ are assumed for the incident field. Forth, the wavelength $\lambda = 1$ is used. Finally, by divide Γ into small segments and using pulse basis functions and the Dirac delta testing function in (7), (7) becomes [9]

$$Z_{mn} \approx \begin{cases} \dfrac{k_0\eta_0}{4} w_n \left[1 - j\dfrac{2}{\pi}\ln\left(\dfrac{1.781\, k_0\, w_n}{4(2.718)}\right)\right], & m = n \\ \dfrac{k_0\eta_0}{4} w_n H_0^{(2)}\left(k_0|\boldsymbol{\rho}_m - \boldsymbol{\rho}_n|\right), & m \ne n \end{cases} \tag{11}$$

where w_n is the size of the nth segment, $\boldsymbol{\rho}_m = x_m\mathbf{a}_x + y_m\mathbf{a}_y$ and $\boldsymbol{\rho}_n = x_n\mathbf{a}_x + y_n\mathbf{a}_y$ denote the center of the mth and nth segments of the observation and the source point respectively. Also, for the same basis and testing functions $E_z^{inc(m)} = E_0 \exp(jk_0(x_m\cos\Phi_i + y_m\sin\Phi_i))$ and $J(\boldsymbol{\rho}_n)\, I_n$. For this case, (10) becomes

$$E_z^{inc}(\rho_m) = \sum_{n=1}^{N} Z_{mn} I_n = \underbrace{\frac{k_0\eta_0}{4} \sum_{n\in|\boldsymbol{\rho}_m-\boldsymbol{\rho}_n|<|\bar{\boldsymbol{\rho}}|} H_0^{(2)}\left(k_0|\boldsymbol{\rho}_m - \boldsymbol{\rho}_n|\right) I_n w_n}_{\text{direct multiplication}} + \frac{k_0\eta_0}{4} \sum_{n_y=-N_y}^{N_y} \sum_{n_x=-N_x}^{N_x} C_{n_y n_x} e^{jn_x\omega_{0_x}x_m} e^{jn_y\omega_{0_y}y_m} \times \underbrace{\sum_{n\in|\boldsymbol{\rho}_m-\boldsymbol{\rho}_n|>|\bar{\boldsymbol{\rho}}|} e^{-jn_x\omega_{0_x}x_n} e^{-jn_y\omega_{0_y}y_n} I_n w_n}_{\text{fast multiplication}}. \tag{12}$$

To show the stability and accuracy of the proposed method, EWS from PEC circular cylinders as an example is used. The analytical solution for it is given by [27]

$$J_i = -\frac{2E_0}{\omega\mu_0\pi a} \sum_{n=-\infty}^{\infty} \frac{j^{-n} e^{jn\theta_i}}{H_n^{(2)}(k_0 a)} \tag{13}$$

where J_i is the induced current at contour angle θ_i, E_0 is the magnitude of the incident field, $\mu_0 = 4\pi\times10^{-7}$ H/m is permeability of vacuum, a is the circular cylinder radius, and $\omega = 2\pi/f$ where f is the frequency used in the problem.

EWS from PEC circular cylinders with radii 1λ m and 2λ m are solved using FS-MoM as a function of N_x and N_y where $N_x = N_y$ is used. For each radius, different number of points $N = 2^8$, 2^9, 2^{10}, 2^{11}, and 2^{12} are used to test the behavior of the method with an increased number of points. Figure 3(a), and 3(b) show the results. It is clear that as the upper limits increase, the MSE reduces. Also, it can be

noted that increasing N does not change much in MSE. This makes sense because the approximation has enough Fourier coefficients to represent the original function. This result is the essence of explaining why FS-MoM reduces the computational complexity. In MoM, as N in the problem increases, the computational complexity will increase in $O(N^2)$ relation which is a square relation. On the other hand, for FS-MoM, after determining the values of the summation limits for the required error, the increases of N will affect the computational complexity in a linear relation as shown in Tab. 1, i.e., $N \times N_{\text{direct}} + (2N_y+1)(2N_x+1) \times [N_{\text{fast}} + 1 + N]$ where $(2N_y+1)(2N_x+1)$ is a constant.

Figure 4 shows the unknown currents versus θ, where θ is the angle along contour of the scatterer for a PEC circular cylinder of radius 2λ m, solved using the analytical solution (13), MoM (11) and FS-MoM (12). The time and memory required to perform MVM between the two methods are shown in Fig. 5 as a function of N. It is clear

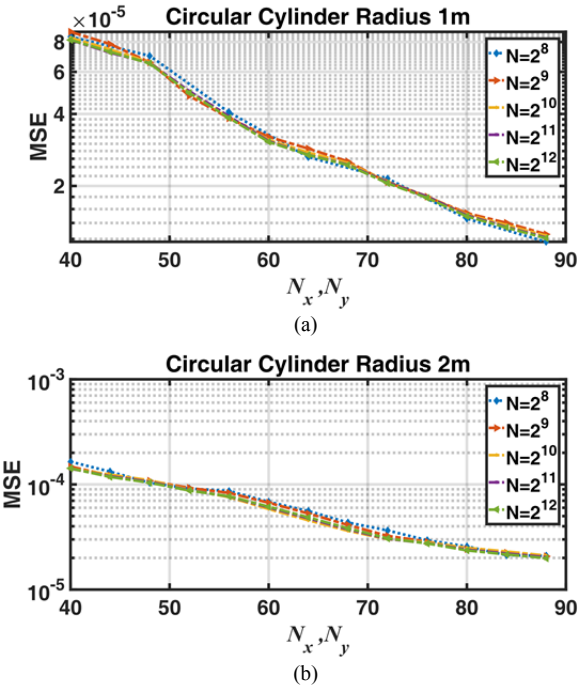

Fig. 3. MSE versus N_x and N_y with points $N = 2^8,2^9,2^{10},2^{11}$, and 2^{12} for PEC circular cylinder with a radius of: (a) 1 m, (b) 2 m.

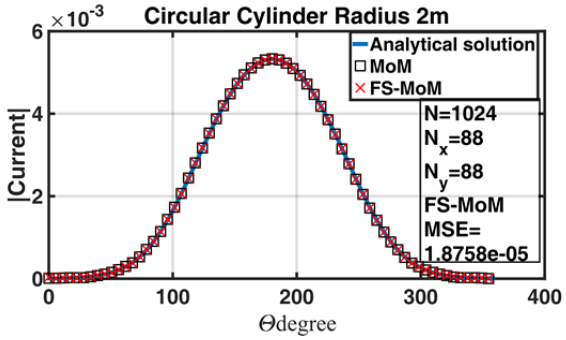

Fig. 4. The unknown current versus the contour angle θ for EWS from a PEC circular cylinder with a radius 2 m using MoM and FS-MoM.

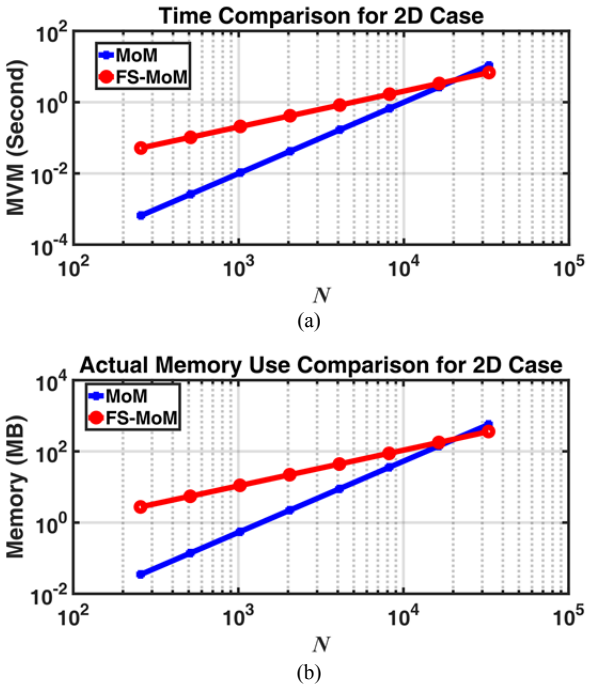

Fig. 5. (a) Time and (b) memory required to perform MVM per iteration for MoM and FS-MoM.

that as N increased, the proposed method becomes faster and uses less memory than the MoM.

4. Conclusions

FS can be used to represent the Green's function, i.e., the zeroth-order Hankel function of the second kind. This representation can be used to reduce the computational complexity of the MoM. The results showed that the proposed method is accurate, efficient, and the most important, it can be used without any mathematical derivation on the Green's function that other methods required. Future work will focus on reducing the computational complexity more by using the FS properties and on studying different approaches to execute the method.

References

[1] HARRINGTON, R. *Field Computation by Moment Method*. Piscataway, NJ (USA): Wiley–IEEE Press, 1993. ISBN-13: 978-0780310148

[2] OLSHANSKII, A., TYRTYSHNIKOV, E. *Iterative Methods for Linear Systems: Theory and Applications*. Philadelphia (USA): SIAM-Society for Industrial and Applied Mathematics, 2014. ISBN: 978-1-61197-345-7

[3] ZHAO, K., VOUVAKIS, M., LEE, J. The adaptive cross-approximation algorithm for accelerated method of moments computations of EMC problems. *IEEE Transactions on Electromagnetic Compatibility*, 2005, vol. 47, no. 4, p. 763–773. DOI: 10.1109/TEMC.2005.857898

[4] SHAEFFER, J. Direct solve of electrically large integral equations for problem sizes to 1M unknowns. *IEEE Transactions on Antennas and Propagation*, 2008, vol. 56, no. 8, p. 2306–2313. DOI: 10.1109/TAP.2008.926739

[5] MICHIELSSEN, E., BOAG, A. A multilevel matrix decomposition algorithm for analyzing scattering from large structures. *IEEE Transactions on Antennas and Propagation*, 1996, vol. 44, no. 8, p. 1086–1093. DOI: 10.1109/8.511816

[6] VOUVAKIS, M., LEE, S., ZHAO, K., et al. A symmetric FEM-IE formulation with a single-level IE-QR algorithm for solving electromagnetic radiation and scattering problems. *IEEE Transactions on Antennas and Propagation*, 2004, vol. AP-52, no. 11, p. 409–418. DOI: 10.1109/TAP.2004.837525

[7] BOJARSKI, N. K-space formulation of the electromagnetic scattering problem. *Air Force Avionics Lab. Technical Report,* Wright-Patterson Air Force Base, Ohio (USA), 1971.

[8] SARKAR, T., ARVAS, E., RAO, S. Application of FFT and the conjugate gradient method for the solution of electromagnetic radiation from electrically large and small conducting bodies. *IEEE Transactions on Antennas and Propagation*, 1986, vol. 34, no. 5, p. 635–640. DOI: 10.1109/TAP.1986.1143871

[9] JIN, J. *Theory and Computation of Electromagnetic Fields*. New Jersey (USA): Wiley & Sons, 2015. ISBN: 978-1-119-10804-7

[10] BLESZYNSKI, E., BLESZYNSKI, M., JAROSZEWICZ, T. A fast integral-equation solver for electromagnetic scattering problems. In *Proceedings of IEEE Antennas and Propagation Society International Symposium and URSI National Radio Science Meeting.* Seattle (WA, USA), Jun. 1994, vol. 1, p. 416–419. DOI: 10.1109/APS.1994.407725

[11] BLESZYNSKI, E., BLESZYNSKI, M., JAROSZEWICZ, T. AIM: Adaptive integral method for solving large-scale electromagnetic scattering and radiation problems. *Radio Science*, 1996, vol. 31, no. 5, p. 1225–1251. DOI: 10.1029/96RS02504

[12] PHILLIPS, J., WHITE, J. A precorrected-FFT method for electrostatic analysis of complicated 3D structures. *IEEE Transactions on Computer-Aided Design of Integrated Circuits and Systems,* 1997, vol. 16, no. 10, p. 1059–1072. DOI: 10.1109/43.662670

[13] NIE, X., LI, L., YUAN, N., et al. Precorrected-FFT solution of the volume integral equation for 3-D inhomogeneous dielectric objects. *IEEE Transactions on Antennas and Propagation*, 2005, vol. 53, no. 1, p. 313–320. DOI: 10.1109/TAP.2004.838803

[14] CHAN, C., LIN, C., TSANG, L., et al. A sparse-matrix/canonical grid method for analyzing microstrip structures. *IEICE Transactions on Electronics*, 1997, vol. E80C, no. 11, p. 1354–1359. ISSN: 0916-8516

[15] SEO, S., WANG, C., LEE, J. Analyzing PEC scattering using an IE-FFT algorithm. *ACES Journal*, 2009 vol. 24, no. 2, p. 116–128.

[16] ROKHLIN, V. Rapid solutions of integral equations of scattering theory in two dimensions. *Journal of Computational Physics*, 1990, vol. 86, no. 2, p. 414–439. DOI: 10.1016/0021-9991(90)90107-C

[17] COIFMAN, R., ROKHLIN, V., WANDZURA, S. The fast multipole method for the wave equation: a pedestrian prescription. *IEEE Antennas and Propagation Magazine*, 1993, vol. 35, no. 3, p. 7–12. DOI: 10.1109/74.250128

[18] CHEW, W., JIN, J., MICHIELSSEN, E., SONG, J., *Fast and Efficient Algorithms in Computational Electromagnetics*. Norwood (USA): Artech House, 2001. ISBN: 1-58053-152-0

[19] CHEW, W., CUI, T., SONG, J. A FAFFA-MLFMA algorithm for electromagnetic scattering. *IEEE Transactions on Antennas and Propagation,* 2002, vol. 50, no. 11, p. 1641–1649. DOI: 10.1109/TAP.2002.802162

[20] VELAMPARAMBIL, S., CHEW, W., SONG, J. 10 million unknowns: Is it that big? [computational electromagnetics]. *IEEE Antennas and Propagation Magazine*, 2003, vol. 45, no. 2, p. 45–58. DOI: 10.1109/MAP.2003.1203119

[21] TZOULIS, A., EIBERT, T. Efficient electromagnetic near-field computation by the multilevel fast multipole method employing mixed nearfield/far-field translations. *IEEE Antennas and Wireless Propagation Letters*, 2005, vol. 4, p. 449–452. DOI: 10.1109/LAWP.2005.860195

[22] TZOULIS, A., EIBER, T. Fast computation of electromagnetic nearfields with the multilevel fast multipole method combining near-field and far-field translations. *Advanced Radio Science*, 2006, vol. 4, p. 111–115. DOI: 10.5194/ars-4-111

[23] SOLÍS, D. M., ARAÚJO, M. G., GARCÍA, S., et al. Multilevel fast multipole algorithm for fields. *Journal of Electromagnetic Waves and Applications*, 2018, vol. 32, no. 10, p. 1261–1274. DOI: 10.1080/09205071.2018.1431155

[24] LIU, Y., SONG, W., WU, D., et al. Fast and accurate calculation of electromagnetic scattering/radiation fields. *IEEE Transactions on Antennas and Propagation*, 2019, vol. 67, no. 11, p. 7168–7173. DOI: 10.1109/TAP.2019.2927618

[25] POULARIKAS, A. *The Handbook Formulas and Tables for Signal Processing*. Florida (USA): CRC Press LLC, 1999. ISBN: 0-8493-8579-2

[26] VOLAKIS, J., SERTEL, K. *Integral Equation Methods for Electromagnetics*. NC (USA): SciTech Publishing, Inc., 2012. ISBN: 978-1-891121-93-7

[27] GARG, R. *Analytical and Computational Methods in Electromagnetics*. MA (USA): Artech House, 2008. ISBN-13: 978-1-59693-385-9